Stanford Exploration Project, Report 120, May 3, 2005, pages 105–124

Stanford Exploration Project, Report 120, May 3, 2005, pages 105–124

3D wavefield extrapolation in laterally-varying tilted TI media

Guojian Shan and Biondo Biondi[1]

ABSTRACT

We develop a new 3D wavefield-extrapolation method for a transversely isotropic (TI) medium with a symmetry axis. The wavefield extrapolation is done by an implicit isotropic extrapolation operator with an explicit correction operator. The explicit correction is a 2D convolution operator in the space domain, whose coefficients are estimated by a weighted least-squares method in the Fourier domain. The extrapolation operator is stable and suitable for laterally-varying 3D TI media. This new method can be used to extrapolate wavefields in a 3D transversely isotropic medium with a vertical symmetry axis (VTI) in tilted coordinates. We also discuss the effects of the filter length on its accuracy and shorten the filter by changing the least-squares weighting function. We present the impulse response of our algorithm and compare it with the anisotropic phase-shift method.

INTRODUCTION

Many rocks are anisotropic, and most sedimentary rocks can be approximated as TI media. If anisotropy is not taken into account in the migration, reflectors, especially steeply dipping reflectors, will be imaged incorrectly. To image the reflector in a TI medium, it is important to use an anisotropic wavefield-extrapolation method. Implicit methods (Ristow and Ruhl, 1997), phase-shift-plus-interpolation (PSPI) (Rousseau, 1997), non-stationary phase-shift (Ferguson and Margrave, 1998), explicit operators (Uzcategui, 1995; Zhang et al., 2001a,b), and reference anisotropic phase-shift with an explicit correction filter (Baumstein and Anderson, 2003) have been developed to extrapolate wavefields in 2D VTI, 3D VTI, or 2D tilted TI media.

Explicit extrapolation operators have proved useful in isotropic wavefield extrapolation (Holberg, 1988; Blacquiere et al., 1989; Thorbecke, 1997). The dispersion relation in a tilted TI medium is very complicated, and it is very difficult to design an implicit extrapolation operator for it. However, explicit operators can still handle in the same way as isotropic media. In 3D, the circular symmetry of the isotropic or VTI media allows us to design a 1D algorithm to replace the 2D convolution operator by McClellen transformations (Hale, 1991b,a; Zhang et al., 2001b). For tilted TI media, the deviation of the symmetry axis from the vertical direction breaks that circular symmetry. As a result, a 2D convolution operator has to be designed for the wavefield extrapolation in 3D tilted TI media.

[1]**email:** shan@sep.stanford.edu, biondo@sep.stanford.edu

Tilted coordinates (Shan and Biondi, 2004a) are used to extrapolate wavefields in a direction close to the wave propagation direction. We can use tilted coordinates to get good accuracy for high-angle energy using a less accurate operator. A VTI medium in Cartesian coordinates becomes a tilted TI medium in tilted coordinates. Thus to extrapolate wavefields in tilted coordinates in a VTI medium, we need an extrapolation operator for tilted TI media.

In this paper, we extrapolate the wavefield in 3D tilted TI media using an implicit isotropic operator with an explicit anisotropic correction (Shan and Biondi, 2004b). We begin by first deriving the 3D dispersion relation in tilted TI media. Then we discuss how to design 2D antisymmetric convolution operators in the Fourier domain for tilted TI media. We discuss how the length of the filter affects the accuracy of the operator and propose a way to design short 2D filters. Finally, we present 3D impulse response for a tilted TI medium of our algorithm.

3D DISPERSION RELATION IN TILTED TI MEDIA

In 3D VTI media, the phase velocity of P- and SV-waves in Thomsen's notation can be expressed as follows (Tsvankin, 1996):

$$\frac{V^2(\theta)}{V_{P0}^2} = 1 + \varepsilon \sin^2(\theta) - \frac{f}{2} \pm \frac{f}{2}\sqrt{\left(1 + \frac{2\varepsilon \sin^2(\theta)}{f}\right)^2 - \frac{2(\varepsilon - \delta)\sin^2(2\theta)}{f}}, \tag{1}$$

where θ is the phase angle of the propagating wave, and $f = 1 - (V_{S0}/V_{P0})^2$. V_{P0} and V_{S0} are the P- and SV- wave velocities in the vertical direction, respectively. The anisotropy parameters ε and δ are defined by Thomsen (1986):

$$\varepsilon = \frac{C_{11} - C_{33}}{2C_{33}}, \delta = \frac{(C_{11} + C_{44})^2 - (C_{33} - C_{44})^2}{2C_{33}(C_{33} - C_{44})},$$

where C_{ij} are elastic moduli. In equation (1), $V(\theta)$ is the P-wave phase-velocity when the sign in front of the square root is positive, and the SV-wave phase velocity for a negative sign. Let k_x', k_y' and k_z' be the wavenumbers for VTI media in Cartesian coordinates. For plane-wave propagation, the phase angle θ is related to the wavenumbers k_x', k_y' and k_z' by the following relations:

$$\sin\theta = \frac{V(\theta)k_r'}{\omega}, \qquad \cos\theta = \frac{V(\theta)k_z'}{\omega}, \tag{2}$$

where ω is the temporal frequency, and $k_r' = \sqrt{(k_x')^2 + (k_y')^2}$. From equations (1) and (2), we can derive the dispersion relation for 3D VTI media as follows:

$$b_6(k_z')^4 + b_5(k_r')^4 + b_4(k_z')^2(k_r')^2 + b_3(k_z')^2 + b_2(k_r')^2 + b_1 = 0, \tag{3}$$

where

$$\begin{aligned} b_6 &= f-1, \\ b_5 &= (f-1)(1+2\varepsilon), \\ b_4 &= 2\big[(f-1)(1+\varepsilon)-f(\varepsilon-\delta)\big], \\ b_3 &= \left(\tfrac{\omega}{v_p}\right)^2(2-f), \\ b_2 &= (2+2\varepsilon-f)\left(\tfrac{\omega}{v_p}\right), \\ b_1 &= \left(\tfrac{\omega}{v_p}\right)^4. \end{aligned} \tag{4}$$

For tilted TI media, the symmetry axis deviates from the vertical direction. We need two angles to describe the tilting direction, the tilting angle φ and the azimuth of the tilting direction ψ. We first assume $\psi = 0$, that is the symmetry axis is in the plane $y = 0$. Then we generalize the dispersion relation to the case that $\psi \neq 0$ by coordinate rotation.

For a tilted TI medium, if we rotate the coordinates so that the symmetry axis is the axis z', it becomes a VTI medium in the new coordinates. Let k_x, k_y, and k_z be the wavenumbers for a tilted TI medium in Cartesian coordinates. k'_x, k'_y and k'_z, which are the wavenumbers for VTI media in Cartesian coordinates, can also be considered as the wavenumbers for tilted TI media in the rotated coordinates. For the case that $\psi = 0$, the dispersion relation can be obtained from equation (3) by rotating the coordinates as follows:

$$\begin{pmatrix} k'_x \\ k'_z \end{pmatrix} = \begin{pmatrix} \cos\varphi & -\sin\varphi \\ \sin\varphi & \sin\varphi \end{pmatrix} \begin{pmatrix} k_x \\ k_z \end{pmatrix}. \tag{5}$$

We can re-organize the the dispersion relation and obtain the equation for the wavenumber k_z as follows:

$$a_4 k_z^4 + a_3 k_z^3 + a_2 k_z^2 + a_1 k_z + a_0 = 0, \tag{6}$$

where

$$\begin{aligned} a_4 &= (f-1) + 2\varepsilon(f-1)\sin^2\varphi - \tfrac{f}{2}(\varepsilon-\delta)\sin^2 2\varphi, \\ a_3 &= 2(f-1)\varepsilon\sin 2\varphi - f(\varepsilon-\delta)\sin 4\varphi, \\ a_2 &= [2(f-1)(1+\varepsilon) - f(\varepsilon-\delta)(2\cos^2 2\varphi - \sin^2 2\varphi)]k_x^2 \\ &+ 2[(f-1)(1+\varepsilon) + (f-1)\varepsilon\sin^2\varphi - f(\varepsilon-\delta)\cos^2\varphi]k_y^2 \\ &+ \left(\tfrac{\omega}{v_{p0}}\right)^2(2\varepsilon\sin^2\varphi + 2 - f), \\ a_1 &= [2(f-1)\varepsilon\sin 2\varphi + f(\varepsilon-\delta)\sin 4\varphi]k_x^3 \\ &+ 2\sin 2\varphi[(f-1)\varepsilon + f(\varepsilon-\delta)]k_x k_y^2 \\ &+ 2\varepsilon\left(\tfrac{\omega}{v_{p0}}\right)^2\sin 2\varphi k_x, \\ a_0 &= [(f-1)(1+2\varepsilon\cos^2\varphi) - \tfrac{f}{2}(\epsilon-\delta)\sin^2 2\varphi]k_x^4 + (f-1)(1+2\varepsilon)k_y^4 \\ &+ 2[(f-1)(1+\varepsilon+\varepsilon\cos^2\varphi) - f(\epsilon-\delta)\sin^2\varphi]k_x^2 k_y^2 \\ &+ \left(\tfrac{\omega}{v_{p0}}\right)^2(2-f+2\varepsilon\cos^2\varphi)k_x^2 + 2\left(\tfrac{\omega}{v_{p0}}\right)^2(2+\varepsilon-f)k_y^2. \end{aligned} \tag{7}$$

Equation (6) is a quartic equation in k_z. Given k_x, k_z, the velocity v_{p0}, the anisotropy parameters ε and δ, and the tilting angle φ, we can calculate all the coefficients of equation (6), and

it can be solved analytically (Abramowitz and Stegun, 1972). Usually there are four solutions for equation (6). Two of them are related to the up- and down-going P-wave, and the other two are related to the up- and down-going SV-wave, respectively.

Let k_x'', k_y'' and k_z'' be the wavenumbers for tilted TI media with a general ψ in the original coordinate system. For general ψ, after solving equation (6), we can get the wavenumber k_z by rotating coordinates (k_x, k_y) as follows:

$$\begin{pmatrix} k_x'' \\ k_y'' \end{pmatrix} = \begin{pmatrix} \cos\psi & -\sin\psi \\ \sin\psi & \sin\psi \end{pmatrix} \begin{pmatrix} k_x \\ k_y \end{pmatrix}. \tag{8}$$

Figure 1 shows k_z as a function of k_x and k_y in a constant tilted TI medium. In this medium, the velocity is 2000 m/s, ε is 0.4, δ is 0.2, φ is $\frac{\pi}{6}$ and ψ is 0. The frequency used in Figure 1 57 Hz.

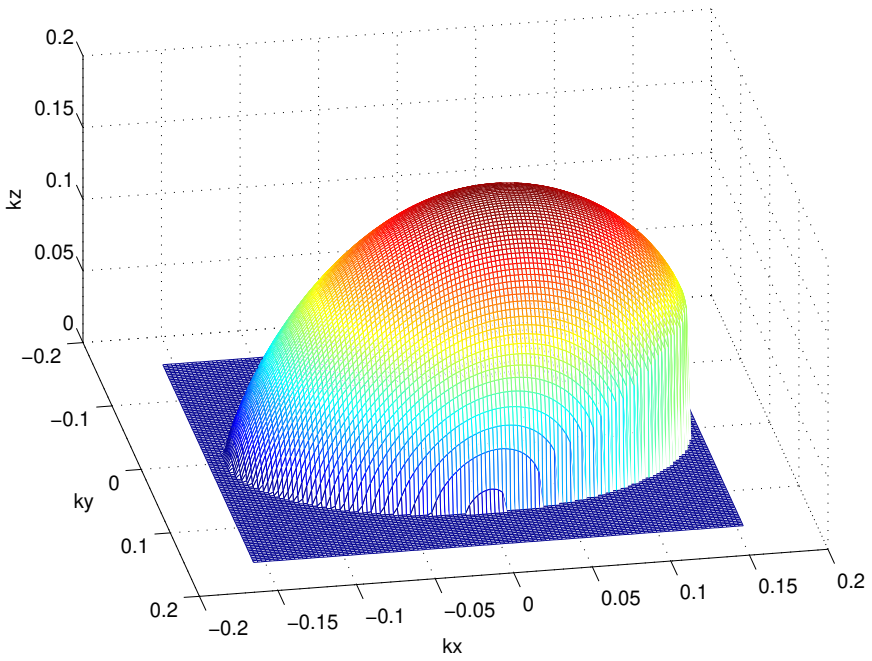

Figure 1: Dispersion relation of 3D tilted TI media. guojian2-dispersion [NR]

WAVEFIELD EXTRAPOLATION OPERATOR

For a homogeneous medium, the wavefield can be extrapolated by an anisotropic phase shift in the Fourier domain as follows:

$$P^{z+1}(k_x, k_y) = P^z(k_x, k_y) e^{k_z \Delta z}. \tag{9}$$

In reality, the velocity and anisotropy parameters change laterally. PSPI, explicit methods, or a combination of PSPI and explicit correction will remedy this problem. We extrapolate the wavefield by an isotropic operator with an explicit correction operator as follows:

$$P^{z+1}(k_x,k_y) = \left[P^z(k_x,k_y) e^{k_z^{iso}\Delta z} \right] e^{(k_z - k_z^{iso})\Delta z}. \tag{10}$$

where $k_z^{iso} = \sqrt{\frac{\omega^2}{V_{P0}^2} - (k_x^2 + k_y^2)}$. In VTI media, the correction operator $e^{(k_z - k_z^{iso})\Delta z}$ is circularly symmetric. This allows us to use a 1D algorithm to replace the 2D operator by McClellan transformations (McClellan and Parks, 1972; McClellan and Chan, 1977; Hale, 1991a). However, tilting the symmetry axis in tilted TI media breaks the circular symmetry. As a result, we need to design a 2D convolution operator in the Fourier domain for wavefield extrapolation in 3D tilted TI media.

The correction operator is not symmetric for axes x or y in tilted TI media. This means

$$F(k_x,k_y) = e^{(k_z(k_x,k_y) - k_z^{iso})\Delta z}$$

is not a even function of k_x and k_y. However, we can decompose the function $F(k_x,k_y)$ into either even or odd functions of k_x and k_y, and approximate the even parts with cosine functions and the odd parts with sine functions.

We can decompose the function $F(k_x,k_y)$ into even and odd parts for the axis k_x by

$$F^e(k_x,k_y) = \frac{1}{2}[F(k_x,k_y) + F(-k_x,k_y)], \tag{11}$$

$$F^o(k_x,k_y) = \frac{1}{2}[F(k_x,k_y) - F(-k_x,k_y)]. \tag{12}$$

We can decompose the operator F^e and F^o into odd or even parts for the axis k_y by

$$F^{ee}(k_x,k_y) = \frac{1}{2}[F^e(k_x,k_y) + F^e(k_x,-k_y)], \tag{13}$$

$$F^{eo}(k_x,k_y) = \frac{1}{2}[F^e(k_x,k_y) - F^e(k_x,-k_y)], \tag{14}$$

$$F^{oe}(k_x,k_y) = \frac{1}{2}[F^o(k_x,k_y) + F^o(k_x,-k_y)], \tag{15}$$

$$F^{oo}(k_x,k_y) = \frac{1}{2}[F^o(k_x,k_y) - F^o(k_x,-k_y)]. \tag{16}$$

The function $F^{ee}(k_x,k_y)$ is an even function of both k_x and k_y, so it can be approximated by

$$F^{ee}(k_x,k_y) = \sum_{n_x,n_y} a^{ee}_{n_x n_y} \cos(n_x \Delta x k_x) \cos(n_y \Delta y k_y), \tag{17}$$

The function $F^{oe}(k_x,k_y)$ is an even function of k_y and an odd function of k_x, so it can be approximated by

$$F^{oe}(k_x,k_y) = \sum_{n_x,n_y} a^{oe}_{n_x n_y} \sin(n_x \Delta x k_x) \cos(n_y \Delta y k_y). \tag{18}$$

The function $F^{eo}(k_x,k_y)$ is an even function of k_x and an odd function of k_y, so it can be approximated by

$$F^{eo}(k_x,k_y)=\sum_{n_x,n_y} a^{eo}_{n_xn_y}\cos(n_x\Delta x k_x)\sin(n_y\Delta y k_y). \tag{19}$$

The function $F^{oo}(k_x,k_y)$ is an odd function of both k_x,k_y, so it can be approximated by

$$F^{oo}(k_x,k_y)=\sum_{n_x,n_y} a^{oo}_{n_xn_y}\sin(n_x\Delta x k_x)\sin(n_y\Delta y k_y). \tag{20}$$

Coefficients $a^{ee}_{n_xn_y}$, $a^{oe}_{n_xn_y}$, $a^{eo}_{n_xn_y}$ and $a^{oo}_{n_xn_y}$ can be estimated by the weighted least-square method (Thorbecke, 1997), which can be solved by QR decomposition (Baumstein and Anderson, 2003; Shan and Biondi, 2004b). Appendix A discusses how to estimate the coefficients $a^{ee}_{n_xn_y}$, $a^{oe}_{n_xn_y}$, $a^{eo}_{n_xn_y}$ and $a^{oo}_{n_xn_y}$ in detail.

The original operator $F(k_x,k_y)$ can be obtained from $F^{ee}(k_x,k_y)$, $F^{eo}(k_x,k_y)$, $F^{oe}(k_x,k_y)$ and $F^{oo}(k_x,k_y)$ by

$$F(k_x,k_y)=F^{ee}(k_x,k_y)+F^{eo}(k_x,k_y)+F^{oe}(k_x,k_y)+F^{oo}(k_x,k_y). \tag{21}$$

Appendix B derives the inverse Fourier transform of the functions $F^{ee}(k_x,k_y)$, $F^{eo}(k_x,k_y)$, $F^{oe}(k_x,k_y)$ and $F^{oo}(k_x,k_y)$, and obtains the inverse Fourier transform of the function $F(k_x,k_y)$ as follows:

$$\mathcal{F}^{-1}\{F(k_x,k_y)\}=\sum_{n_x,n_y} c_{n_x,n_y}\delta(x+n_x\Delta x,y+n_y\Delta y), \tag{22}$$

where

$$n_x=-N_x,-N_x+1,\cdots,-1,0,1,\cdots,N_x-1,N_x,$$

$$n_y=-N_y,-N_y+1,\cdots,-1,0,1,\cdots,N_y-1,N_y,$$

and c_{n_x,n_y} is as follows:

$$c_{00}=a^{ee}_{00}, \tag{23}$$

$$c_{n_x,n_y}=\frac{1}{4}\left[\left(a^{ee}_{n_xn_y}-a^{oo}_{n_xn_y}\right)+i\left(a^{eo}_{n_xn_y}+a^{oe}_{n_xn_y}\right)\right], \quad \text{if } n_x>0 \text{ and } n_y>0 \tag{24}$$

$$c_{n_x,n_y}=\frac{1}{4}\left[\left(a^{ee}_{n_xn_y}+a^{oo}_{n_xn_y}\right)+i\left(a^{eo}_{n_xn_y}-a^{oe}_{n_xn_y}\right)\right], \quad \text{if } n_x<0 \text{ and } n_y>0, \tag{25}$$

$$c_{n_x,n_y}=\frac{1}{4}\left[\left(a^{ee}_{n_xn_y}+a^{oo}_{n_xn_y}\right)+i\left(-a^{eo}_{n_xn_y}+a^{oe}_{n_xn_y}\right)\right], \quad \text{if } n_x>0 \text{ and } n_y<0 \tag{26}$$

$$c_{n_x,n_y}=\frac{1}{4}\left[\left(a^{ee}_{n_xn_y}-a^{oo}_{n_xn_y}\right)-i\left(a^{eo}_{n_xn_y}+a^{oe}_{n_xn_y}\right)\right]. \quad \text{if } n_x<0 \text{ and } n_y<0 \tag{27}$$

Let $P^z(x,y)$ be the inverse Fourier transform of $P^z(k_x,k_y)$. It is well known that

$$\delta(x+n_x\Delta x,y+n_y\Delta y)**P^z(x,y)=P^z(x+n_x\Delta x,y+n_y\Delta y),$$

where "$**$" is 2D convolution. From the Fourier transform theory, we have

$$\mathcal{F}^{-1}\{F(k_x,k_y)P^z(k_x,k_y)\} = \mathcal{F}^{-1}\{F(k_x,k_y)\} ** P^z(x,y). \tag{28}$$

Therefore, we can apply the correction operator on the wavefield in the space domain as follows:

$$\mathcal{F}^{-1}\{F(k_x,k_y)\} ** P^z(x,y) = \sum_{n_x,n_y} c_{n_x,n_y} P^z(x+n_x\Delta x, y+n_y\Delta y). \tag{29}$$

From the above derivation, we know that the correction operator is designed in the Fourier domain and is implemented as a convolution in the space domain. For a laterally varying medium, we build a table of the convolution coefficients. When we run wavefield extrapolation, for each space position, we search for the corresponding convolution coefficients from that table and convolve the wavefield with these coefficients at that space position.

FILTER LENGTH, COST, AND ACCURACY

For 3D tilted TI media, the explicit correction operator is a 2D convolution operator. For a medium with lateral variation, a table of the convolution coefficients c_{n_x,n_y} are calculated before the wavefield extrapolation. Long filters can extrapolate high-angle energy accurately. However, it is too expensive to run a 2D convolution filter as long as 19 points in both the x and y directions. Furthermore, it is not practical to store such a big table in the memory. By the weighted least-square method, we can shorten the filter length at the price of losing accuracy for the high-angle energy.

We test a 2D example to check how the length of a filter affects its accuracy. The medium is homogeneous, in which the P-wave velocity in the direction parallel to the symmetry axis is 2000m/s, $\varepsilon = 0.4$, $\delta = 0.2$ and $\varphi = \frac{\pi}{6}$. The frequency is 45.0 Hz.

Let k_x^{max} be the beginning wavenumber for the evanescent energy. We assign a weight of 1 to the wavenumbers smaller than k_x^{max} and a weight of 0.001 to the wavenumbers bigger than k_x^{max}. In Figure 2, the phase for the even part of the 19-point filter example is very close to the true operator. In this model, the beginning wavenumber for the evanescent energy k_x^{max} is 0.15. In Figure 3, the phase curve for the even part of the 5-point filter oscillates around the true operator. The 5-point filter is not accurate even for the low wavenumber energy. If our aim is to guarantee the accuracy of the low-angle (low-wavenumber) energy, we can assign big weights to the low-angle energy but small weights to the high-angle energy. We can also smooth the amplitude and phase of the high angle-energy. Now we assign a weight of 1 to the wavenumbers smaller than $\frac{5}{6}k_x^{max}$ and a weight of 0.001 to the wavenumbers bigger than $\frac{5}{6}k_x^{max}$. In this model, $\frac{5}{6}k_x^{max}$ is 0.125. Figure 4 shows the phase curve of the 5-point filter after we change the weighting policy. The new 5-point filter is very close to the true operator at the low wavenumbers (smaller than 0.12) but has a big error at the high wavenumbers.

Though we lose the accuracy of high-angle energy when shorten the filter when we shorten the filter, we greatly improve the efficiency of our algorithm. If we use the 5-point filter in both

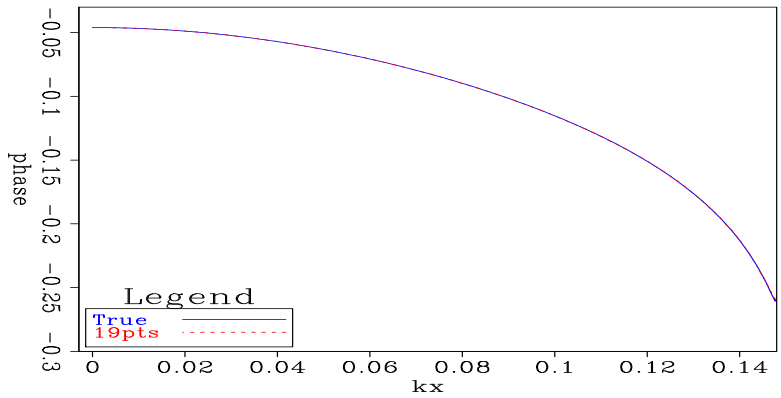

Figure 2: Comparison between the phase curves for the even part of the 19-point filter and the true operator. The continuous curve is the phase of the true operator and the dashed line is the phase of the 19-point filter. guojian2-approx19 [ER]

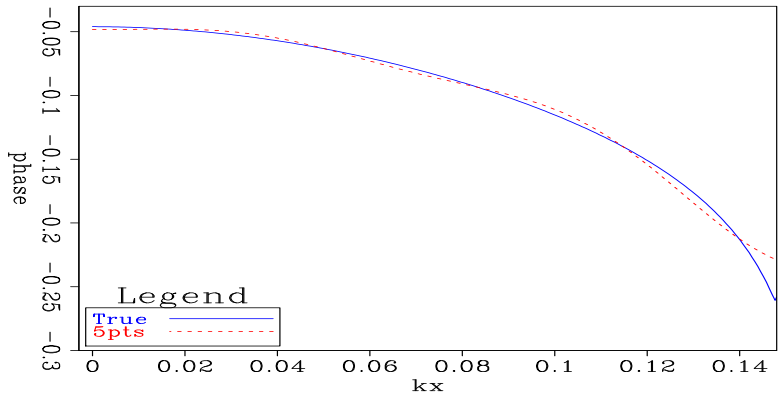

Figure 3: Comparison between the phase curves for the even part of the 5-point filter and the true operator. The continuous curve is the phase of the true operator and the dashed line is the phase of the 5-point filter. guojian2-approx5 [ER]

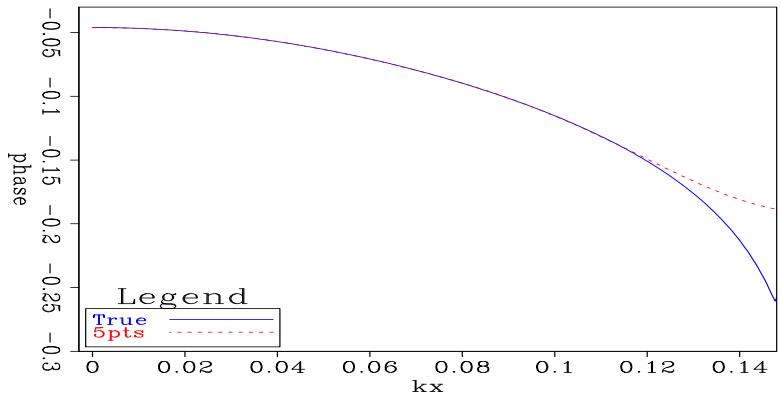

Figure 4: Comparison between the phase curves for the even part of the new 5-point filter and the true operator. The continuous curve is the phase of the true operator and the dashed line is the phase of the new 5-point filter. guojian2-approxw5 [ER]

inline and crossline directions in 3D wavefield extrapolation, the correction operator is a 9×9 2D filter, while it is a 37×37 2D filter if we use the 19-point filter. Therefore using the 5-pointer filter, computation cost for the convolution in 3D wavefield extrapolation is about $\frac{1}{16}$ the cost using the 19-pointer filter. Furthermore, when the media is not homogeneous, searching for the coefficients of a filter in the coefficient table plays an important role in 3D. The total size of the coefficient table of the 5-point filter is about $\frac{1}{16}$ the size of the 19-point filter in 3D. If we build the table with 100 discrete ω/V_{P0}s, 10 discrete εs and 10 discrete δs, the size of table is about 8 Megabyte for the 5-point filter and is about 128 Megabyte for the 19-point filter. The speed of searching in a 8 Megabyte is much faster than that in a 128 Megabyte table. By shortening the filter, we can greatly reduce the cost for the explicit correction operator in 3D wavefield extrapolation.

We lose the accuracy of high-angle energy when we shorten the length of the filter. But we can apply plane-wave decomposition and tilted coordinates (Shan and Biondi, 2004a) to make the wavefield-extrapolation direction close to the direction of wave propagation. By doing this, we can get good accuracy for the high-angle energy even with a less accurate operator.

NUMERICAL EXAMPLE

We first compare the 19-point filter and the improved 5-point filter using a 2D impulse response and a 2D synthetic dataset example. Then we show the 3D impulse responses for the improved 5-point filter and compare them with the impulse response of the anisotropic phase-shift method.

2D impulse response

Figure 5 compares the impulse response of the 19-point filter with that of the improved 5-point filter. The medium of the impulse response is a homogeneous medium, in which the velocity is 2000 m/s, the anisotropy parameters $\varepsilon = 0.4$ and $\delta = 0.2$, and the tilting angle $\varphi = \frac{\pi}{6}$. The travel time for the three impulse are 0.4 s, 0.6 s and 0.8 s, respectively. From Figure 5, we can see that the impulse response of the improved 5-point filter is very similar to that of the 19-point filter at low-angle energy but is different from the 19-point filter at high-angle energy. The improved 5-point filter is accurate for the energy up to 50° in the impulse response, compared to the 19-point filter.

A synthetic anisotropic dataset

Figure 6 compares the 19-point filter with the new 5-point filter for the migration of an anisotropic synthetic dataset. Shan and Biondi (2005) migrate this dataset with the anisotropic plane-wave migration in tilted coordinates. Figure 6(a) shows the density model of this synthetic dataset. We can see the steeply dipping salt flank in the density model. Figure 6(b) is the anisotropic plane-wave migration in tilted coordinates with the 19-point filter. Figure 6(c)

is the anisotropic plane-wave migration in tilted coordinates with the improved 5-point filter. The migration result of the new 5-point filter is very close to the 19-point filter, though it loses a little resolution at the salt flank. This synthetic data example shows that we can get good accuracy for high-angle energy in tilted coordinates, though we use the improved 5-point filter, which is less accurate than 19-point filter.

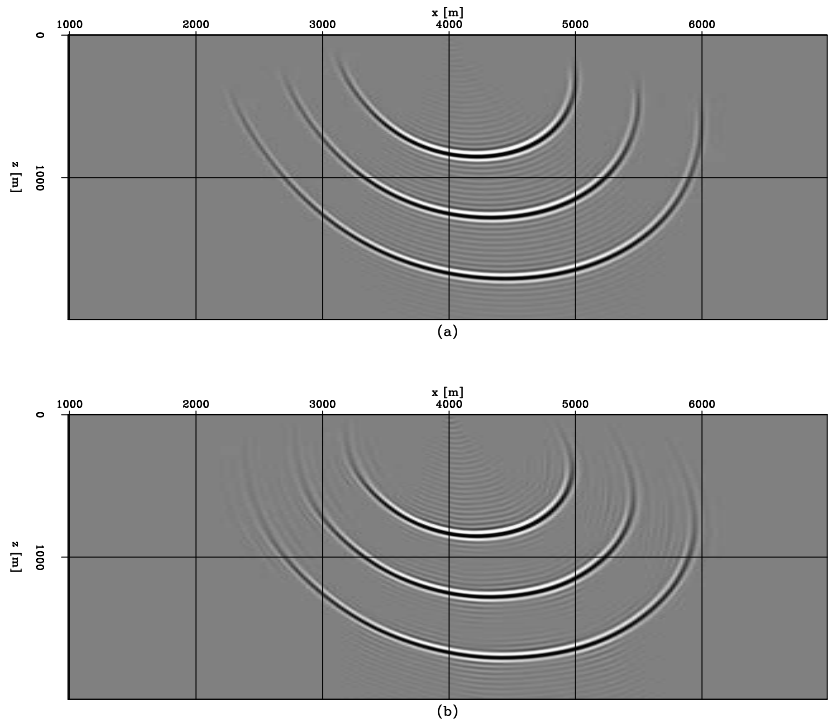

Figure 5: Comparison of the 2D impulse response of the 19-point filter and the improved 5-point filter. (a) The impulse response of the 19-point filter. (b) The impulse response of the improved 5-point filter. guojian2-oldnew [CR]

3D impulse response

Figures 7-9 compare the impulse responses of our algorithm with those of anisotropic phase shift method. The medium is a homogeneous, tilted TI medium. The symmetry axis of the medium is in the (x,z) plane and is tilted 30° from the vertical direction. The P-wave velocity in the direction parallel to the symmetry axis is 2000 m/s. The anisotropy parameters ε and δ are 0.4 and 0.2, respectively. The location of the impulse is at $x = 2000$ m and $y = 2000$ m. The travel time for the three impulses are 0.4 s, 0.6 s and 0.8 s, respectively. Figure 7 shows a depth slice of the impulse responses at $z = 1500$ m. Figure 7(a) is obtained with our algorithm and Figure 7(b) is obtained with the anisotropic phase-shift method. First, Figure 7(a) is very similar to 7(b). Second, the depth slice of the impulse response is not a circle. The wave propagates faster in y than in x direction. Third, the impulse location $x = 2000$ m and $y = 2000$ m is not the center of the impulse response. The impulse response is symmetric along $y = 2000$m, but it is not symmetric along $x = 2000$ m. Figure 8 shows an in-line slice of

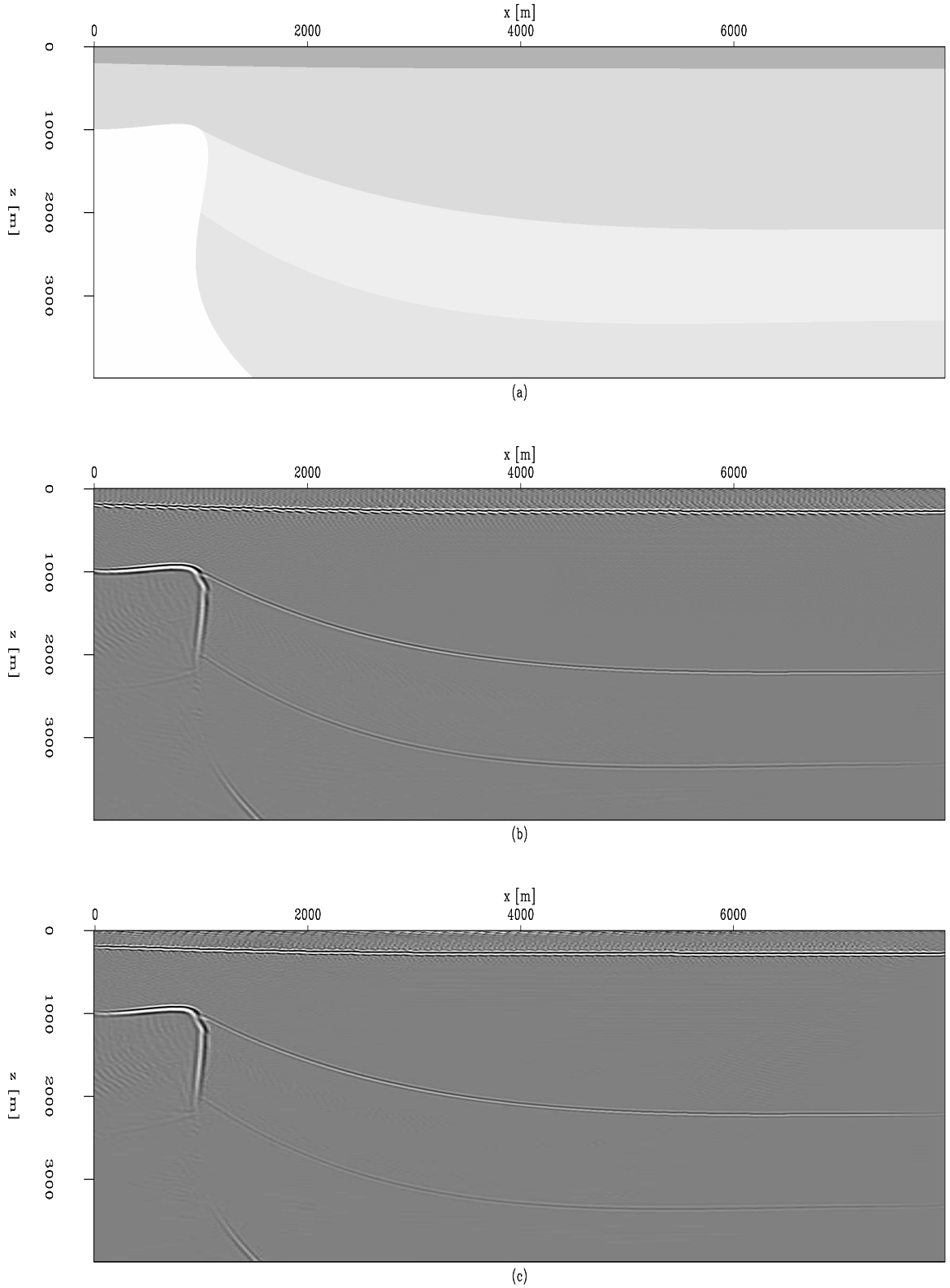

Figure 6: Comparison of the anisotropic plane-wave migration of a synthetic dataset by the 19-point filter and the new 5-point filter. (a) The density model. (b) The migration result of the 19-point filter. (c) The migration result of the new 5-point filter. guojian2-filtercom [CR]

the impulse responses at $y = 2000$ m. Figure 8(a) is obtained with our algorithm and Figure 8(b) is obtained with the anisotropic phase-shift method. Figure 9 shows a cross-line slice of the impulse responses at $x = 2000$ m. Figure 9(a) is obtained with our algorithm and Figure 9(b) is obtained with the anisotropic phase-shift method. From Figure 8 and 9, we can see that the impulse of our algorithm is very close to that of the anisotropic phase-shift method at low-angle energy and is different from the the anisotropic phase-shift method at high-angle energy. Since the medium is homogeneous, the anisotropic phase-shift method is accurate. So our algorithm is accurate for the energy up to 50° in the impulse response, compared to the anisotropic phase-shift method.

CONCLUSION

We present a 3D wavefield-extrapolation algorithm for tilted TI media. The wavefield is extrapolated by an implicit isotropic operator with an explicit anisotropic correction. Tilted TI media are not circularly symmetric, therefore the explicit anisotropic correction has to be a 2D convolution operator. It is designed by a weighed least-square method. With proper weights, we can shorten the correction operator and reduce the computation cost at the price of losing the accuracy of high-angle energy. A 2D synthetic dataset example shows that we can still have good accuracy for high-angle energy by decomposing the wavefields into plane waves and extrapolating them in tilted coordinates. 3D impulse responses show that our algorithm is accurate up to 50° with the short 2D filter.

ACKNOWLEDGMENTS

We would like to thank ExxonMobil for making the synthetic data available.

REFERENCES

Abramowitz, M., and Stegun, I., 1972, Solutions of quartic equations *in* Handbook of Mathematical Functions with Formulas, Graphs, and Mathematical Tables. New York: Dover., 17–18.

Baumstein, A., and Anderson, J., 2003, Wavefield extrapolation in laterally varying VTI media *in* 73rd Ann. Internat. Mtg. Soc. of Expl. Geophys., 945–948.

Blacquiere, G., Debeye, H. W. J., Wapenaar, C. P. A., and Berkhout, A. J., 1989, 3D table-driven migration: Geophys. Prosp., **37**, 925–958.

Ferguson, R. J., and Margrave, G. F., 1998, Depth migration in TI media by nonstationary phase shift *in* 68th Ann. Internat. Mtg. Soc. of Expl. Geophys., 1831–1834.

Hale, D., 1991a, 3-D depth migration via McClellan transformations: Geophysics, **56**, 1778–1785.

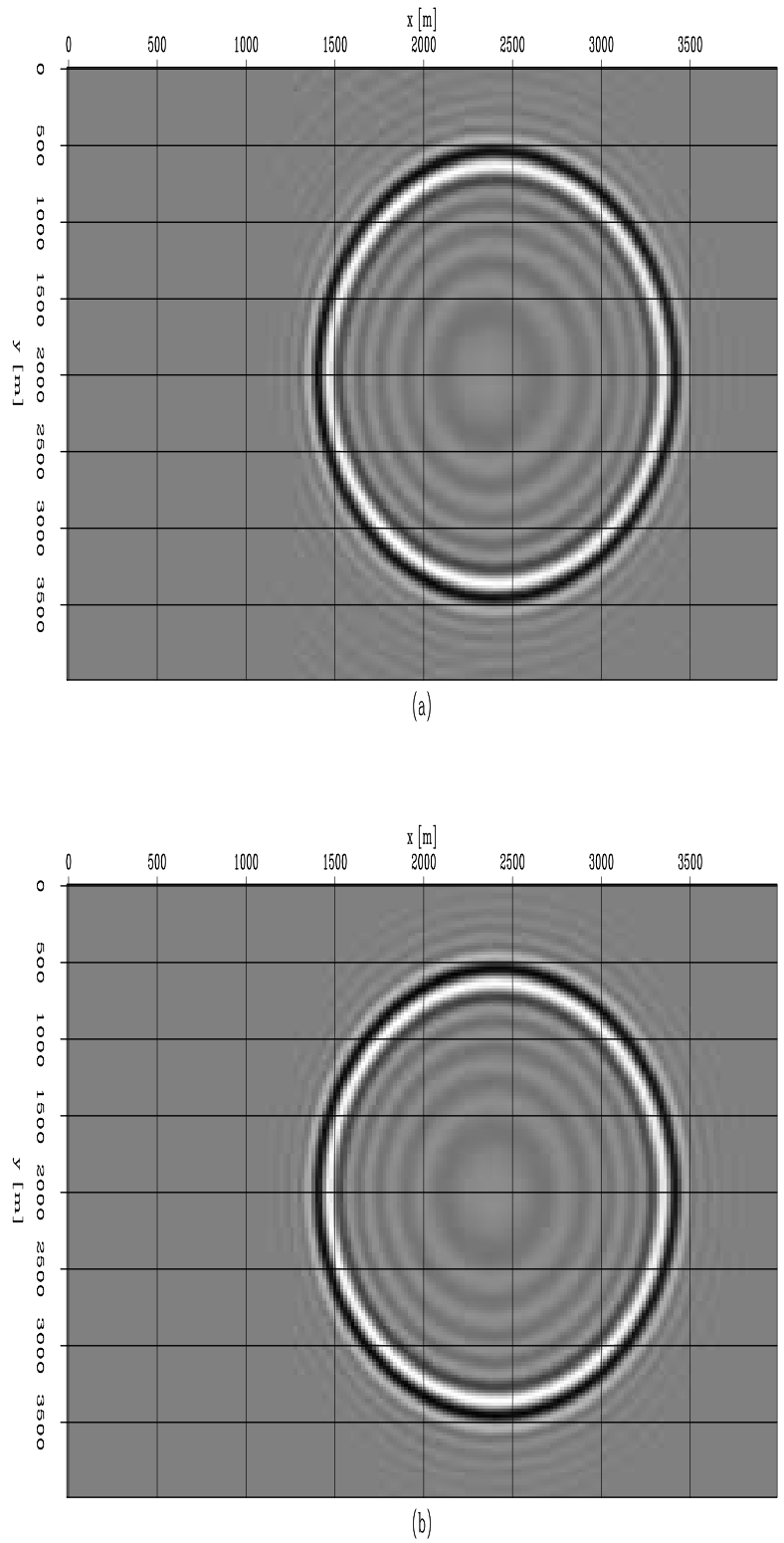

Figure 7: A horizontal slice of the 3D impulse response in a tilted TI medium at a depth of $z = 1000$ m: (a) Our algorithm. (b) The anisotropic phase-shift method. guojian2-depth [CR]

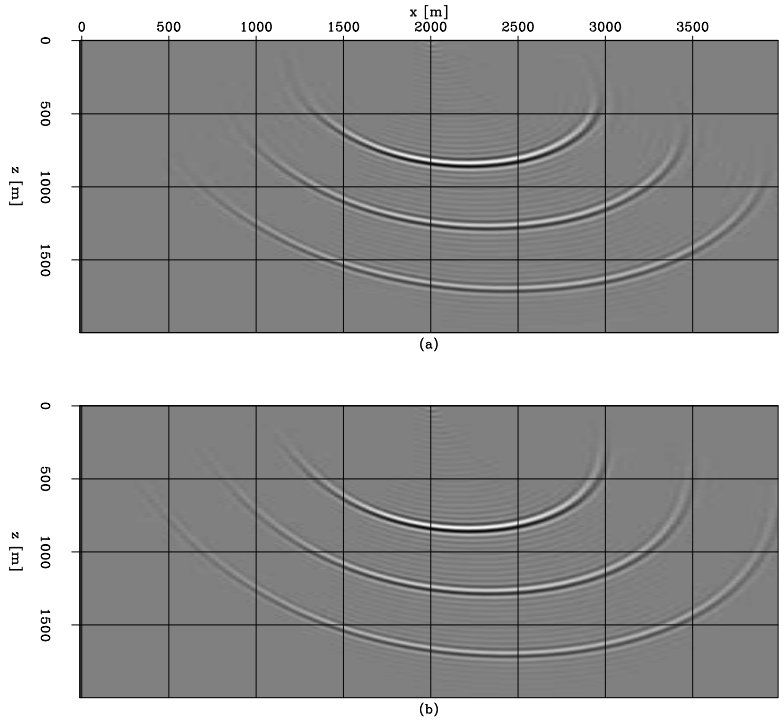

Figure 8: An inline slice of the 3D impulse response in a tilted TI medium at $y = 2000$ m: (a) Our algorithm. (b) The anisotropic phase-shift method. guojian2-inline [CR]

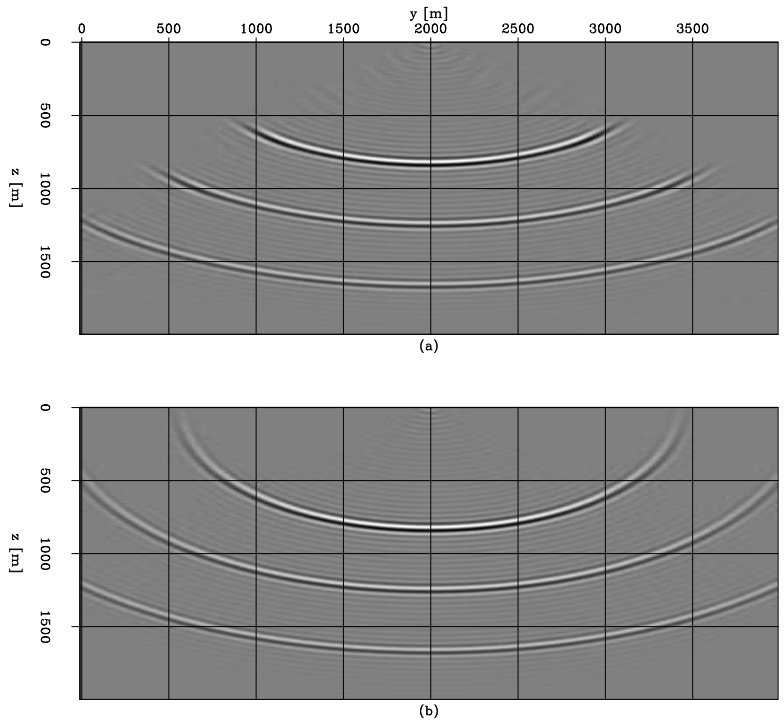

Figure 9: A cross-line slice of the 3D impulse response in a tilted TI medium at $x = 2000$ m: (a) Our algorithm. (b) The anisotropic phase-shift method. guojian2-cross [CR]

—, 1991b, Stable explicit depth extrapolation of seismic wavefields: Geophysics, **56**, 1770–1777.

Holberg, O., 1988, Towards optimum one-way wave propagation: Geophys. Prosp., **36**, 99–114.

McClellan, J., and Chan, D., 1977, A 2-D FIR filter structure derived from the Chebychev recursion: IEEE Trans. Circuits Syst.,, **CAS-24**, 372–378.

McClellan, J. H., and Parks, T. W., 1972, Equiripple approximation of fan filters: Geophysics, **37**, 573–583.

Ristow, D., and Ruhl, T., 1997, Migration in transversely isotropic media using implicit operators *in* 67th Ann. Internat. Mtg. Soc. of Expl. Geophys., 1699–1702.

Rousseau, J. H. L., 1997, Depth migration in heterogeneous, transversely isotropic media with the phase-shift-plus-interpolation method *in* 67th Ann. Internat. Mtg. Soc. of Expl. Geophys., 1703–1706.

Shan, G., and Biondi, B., 2004a, Imaging overturned waves by plane-wave migration in tilted coordinates: 74th Ann. Internat. Mtg., Soc. of Expl. Geophys., Expanded Abstracts, 969–972.

—, 2004b, Wavefield extrapolation in laterally-varying tilted TI media: SEP– **117**, 1–10.

—, 2005, Imaging steeply dipping reflectors in TI media by wavefield extrapolation: SEP–**120**, 63–76.

Thomsen, L., 1986, Weak elastic anisotropy: Geophysics, **51**, 1954–1966.

Thorbecke, J., 1997, Common focus point technology *in* Ph.D. thesis. Delft University of Technology.

Tsvankin, I., 1996, P-wave signatures and notation for transversely isotropic media: An overview: Geophysics, **61**, 467–483.

Uzcategui, O., 1995, 2-D depth migration in transversely isotropic media using explicit operators: Geophysics, **60**, 1819–1829.

Zhang, J., Verschuur, D. J., and Wapenaar, C. P. A., 2001a, Depth migration of shot records in heterogeneous, tranversely isotropic media using optimum explicit operators: Geophys. Prosp., **49**, 287–299.

Zhang, J., Wapenaar, C., and Verschuur, D., 2001b, 3-D depth migration in VTI media with explicit extrapolation operators *in* 71st Ann. Internat. Mtg. Soc. of Expl. Geophys., 1085–1088.

APPENDIX A

This appendix discusses how to estimate the coefficients $a^{ee}_{n_x n_y}$, $a^{oe}_{n_x n_y}$, $a^{eo}_{n_x n_y}$ and $a^{oo}_{n_x n_y}$ in equations (17)-(20).

We begin with equation (17), as the other three equations are silimiar. Let Δk_x and Δk_y be the sampling of the wavenumbers k_x and k_y, respectively. To mimic the behavior of the orginal operator F^{ee}, we need to estimate $a^{ee}_{n_x n_y}$, so that

$$F^{ee}(k_x,k_y) \approx \sum_{n_x,n_y} a^{ee}_{n_x n_y} \cos(n_x \Delta x k_x) \cos(n_y \Delta y k_y),$$

for $k_x \in [0, k_x^{Nyquist}]$ and $k_y \in [0, k_y^{Nyquist}]$, where $k_x^{Nyquist}$ is the Nyquist wavenumber $\frac{\pi}{\Delta x}$ and $k_x^{Nyquist}$ is the Nyquist wavenumber $\frac{\pi}{\Delta y}$. Let M_x be $k_x^{Nyquist}/\Delta k_x$ and M_y be $k_y^{Nyquist}/\Delta k_y$. The coefficients can be estimated by the following fitting goals:

$$\mathbf{W}(\mathbf{A^{ee}}\mathbf{a^{ee}} - \mathbf{f^{ee}}) \approx \mathbf{0}, \tag{A-1}$$

where

$$\mathbf{a^{ee}} = \left(a^{ee}_{00}, a^{ee}_{10}, \cdots, a^{ee}_{n_x-1,n_y}, a^{ee}_{n_x,n_y}, a^{ee}_{n_x+1,n_y}, \cdots, a^{ee}_{N_x,N_y}\right)^T.$$

$\mathbf{A^{ee}}$ is a matrix with the elements

$$A^{ee}_{mn} = \cos(m_x n_x \Delta k_x \Delta x) \cos(m_y n_y \Delta k_y \Delta y),$$

where $m = m_y(M_x+1)+m_x$ and $n = n_y(N_x+1)+n_x$. $\mathbf{f^{ee}}$ is a vector as follows

$$\mathbf{f^{ee}} = \left(f^{ee}_{00}, f^{ee}_{10}, \cdots, f^{ee}_{m_x-1,m_y}, a^{ee}_{m_x,m_y}, f^{ee}_{m_x+1,m_y}, \cdots, f^{ee}_{M_x,M_y}\right)^T,$$

where $f^{ee}_{m_x,m_y} = F^{ee}(m_x \Delta k_x, m_y \Delta k_y)$. $\mathbf{W}$ is a diagonal matrix with the weights for the wavenumbers k_x, k_y. High weights are assigned to the wavenumbers of interest. The wavenumbers, such as the evacent energy, are not of interest and are assigned low weights. Given the same weight matrix $\mathbf{W}$, the matrix $\mathbf{WA^{ee}}$ are same though f^{ee} changes with the function $F^{ee}(k_x,k_y)$. Therefore, QR decomposition is a good way to solve the fitting goal (A-1). First, we run QR decomposition on matrix $\mathbf{WA}$: $\mathbf{WA} = \mathbf{QR}$, where $\mathbf{Q}$ is an orthogonal matrix and $\mathbf{R}$ is an upper triangular matrix. We write down the matrixes $\mathbf{Q}$ and $\mathbf{R}$. Given the function $F^{ee}(k_x,k_y)$, we caluculate $\mathbf{f^{ee}}$. The solution of fitting goal (A-1) $\mathbf{a^{ee}}$ is given by

$$\mathbf{a^{ee}} = \mathbf{R}^{-1}\mathbf{Q}^T\mathbf{W}\mathbf{f^{ee}}. \tag{A-2}$$

For equation (18), we have the following fitting goal:

$$\mathbf{W}(\mathbf{A^{oe}}\mathbf{a^{oe}} - \mathbf{f^{oe}}) \approx \mathbf{0}, \tag{A-3}$$

where

$$\mathbf{a^{oe}} = \left(a^{oe}_{00}, a^{oe}_{10}, \cdots, a^{oe}_{n_x-1,n_y}, a^{oe}_{n_x,n_y}, a^{oe}_{n_x+1,n_y}, \cdots, a^{oe}_{N_x,N_y}\right)^T,$$

and $\mathbf{f^{oe}}$ in equation (A-3) is

$$\mathbf{f^{oe}} = \left(f^{oe}_{00}, f^{oe}_{10}, \cdots, f^{oe}_{m_x-1,m_y}, a^{oe}_{m_x,m_y}, f^{oe}_{m_x+1,m_y}, \cdots, f^{oe}_{M_x,M_y}\right)^T,$$

where $f^{oe}_{m_x,m_y} = F^{oe}(m_x\Delta k_x, m_y\Delta k_y)$. $\mathbf{A^{oe}}$ in equation (A-3) is a matrix with the elements

$$A^{oe}_{mn} = \sin(m_x n_x \Delta k_x \Delta x)\cos(m_y n_y \Delta k_y \Delta y),$$

where $m = m_y(M_x+1)+m_x$ and $n = n_y(N_x+1)+n_x$. For equation (19), we have the following fitting goal:

$$\mathbf{W}(\mathbf{A^{eo}}\mathbf{a^{eo}} - \mathbf{f^{eo}}) \approx \mathbf{0}, \tag{A-4}$$

where

$$\mathbf{a^{eo}} = \left(a^{eo}_{00}, a^{eo}_{10}, \cdots, a^{eo}_{n_x-1,n_y}, a^{eo}_{n_x,n_y}, a^{eo}_{n_x+1,n_y}, \cdots, a^{eo}_{N_x,N_y}\right)^T,$$

and $\mathbf{f^{eo}}$ in equation (A-3) is

$$\mathbf{f^{eo}} = \left(f^{eo}_{00}, f^{eo}_{10}, \cdots, f^{eo}_{m_x-1,m_y}, a^{eo}_{m_x,m_y}, f^{eo}_{m_x+1,m_y}, \cdots, f^{eo}_{M_x,M_y}\right)^T,$$

where $f^{eo}_{m_x,m_y} = F^{eo}(m_x\Delta k_x, m_y\Delta k_y)$. $\mathbf{A^{eo}}$ in equation (A-4) is a matrix with the elements

$$A^{eo}_{mn} = \cos(m_x n_x \Delta k_x \Delta x)\sin(m_y n_y \Delta k_y \Delta y),$$

where $m = m_y(M_x+1)+m_x$ and $n = n_y(N_x+1)+n_x$. For equation (20), we have the following fitting goal:

$$\mathbf{W}(\mathbf{A^{oo}}\mathbf{a^{oo}} - \mathbf{f^{oo}}) \approx \mathbf{0}, \tag{A-5}$$

where

$$\mathbf{a^{oo}} = \left(a^{oo}_{00}, a^{oo}_{10}, \cdots, a^{oo}_{n_x-1,n_y}, a^{oo}_{n_x,n_y}, a^{oo}_{n_x+1,n_y}, \cdots, a^{oo}_{N_x,N_y}\right)^T,$$

and $\mathbf{f^{oo}}$ in equation (A-3) is

$$\mathbf{f^{oo}} = \left(f^{oo}_{00}, f^{oo}_{10}, \cdots, f^{oo}_{m_x-1,m_y}, a^{oo}_{m_x,m_y}, f^{oo}_{m_x+1,m_y}, \cdots, f^{oo}_{M_x,M_y}\right)^T,$$

where $f^{oo}_{m_x,m_y} = F^{oo}(m_x\Delta k_x, m_y\Delta k_y)$. $\mathbf{A^{oo}}$ in equation (A-5) is a matrix with the elements

$$A^{oo}_{mn} = \sin(m_x n_x \Delta k_x \Delta x)\sin(m_y n_y \Delta k_y \Delta y),$$

where $m = m_y(M_x+1)+m_x$ and $n = n_y(N_x+1)+n_x$. Fitting goals (A-3), (A-4), and (A-5) can be solved in the same way as equation (A-1). The solution of fitting goal (A-3), (A-4), (A-5) are given by

$$\mathbf{a^{oe}} = (\mathbf{R^{oe}})^{-1}(\mathbf{Q^{oe}})^T\mathbf{W}\mathbf{f^{oe}}, \tag{A-6}$$

$$\mathbf{a^{eo}} = (\mathbf{R^{eo}})^{-1}(\mathbf{Q^{eo}})^T\mathbf{W}\mathbf{f^{eo}}, \tag{A-7}$$

$$\mathbf{a^{oo}} = (\mathbf{R^{oo}})^{-1}(\mathbf{Q^{oo}})^T\mathbf{W}\mathbf{f^{oo}}, \tag{A-8}$$

where $\mathbf{Q^{oe}}$, $\mathbf{R^{oe}}$, $\mathbf{Q^{eo}}$, $\mathbf{R^{eo}}$ and $\mathbf{Q^{oo}}$, $\mathbf{R^{oo}}$ are the QR decomposition result of the matrixs $\mathbf{WA^{oe}}$, $\mathbf{WA^{eo}}$ and $\mathbf{WA^{oo}}$, respectively.

APPENDIX B

In this appendix, we derive the inverse Fourier transform of the correction operator $F(k_x,k_y)$.

It is well known that the inverse Fourier transform of the function $\cos n_x\Delta x k_x$, $\sin n_x\Delta x k_x$, $\cos n_y\Delta y k_y$, $\sin n_y\Delta y k_y$ are:

$$\mathcal{F}^{-1}\{\cos(n_x\Delta x k_x)\} = \frac{1}{2}(\delta(x-n_x\Delta x)+\delta(x+n_x\Delta x)), \quad \text{(B-1)}$$

$$\mathcal{F}^{-1}\{\sin(n_x\Delta x k_x)\} = \frac{1}{2i}(\delta(x-n_x\Delta x)-\delta(x+n_x\Delta x)), \quad \text{(B-2)}$$

$$\mathcal{F}^{-1}\{\cos(n_y\Delta y k_y)\} = \frac{1}{2}(\delta(y-n_y\Delta y)+\delta(y+n_y\Delta y)), \quad \text{(B-3)}$$

$$\mathcal{F}^{-1}\{\sin(n_y\Delta y k_y)\} = \frac{1}{2i}(\delta(y-n_y\Delta y)-\delta(y+n_y\Delta y)). \quad \text{(B-4)}$$

Let $\delta_{\pm n_x}=\delta(x\pm n_x\Delta x)$, $\delta_{\pm n_y}=\delta(y\pm n_y\Delta y)$ and $\delta_{\pm n_x,\pm n_y}=\delta(x\pm n_x\Delta x, y\pm n_y\Delta y)$. The inverse Fourier transform of the function $\cos(n_x\Delta x k_x)\cos(n_y\Delta y k_y)$ is :

$$\mathcal{F}^{-1}\{\cos(n_x\Delta x k_x)\cos(n_y\Delta y k_y)\} = \frac{1}{4}(\delta_{-n_x}+\delta_{+n_x})*(\delta_{-n_y}+\delta_{+n_y}) \quad \text{(B-5)}$$

$$= \frac{1}{4}(\delta_{-n_x,-n_y}+\delta_{-n_x,+n_y}+\delta_{+n_x,-n_y}+\delta_{+n_x,+n_y}). \quad \text{(B-6)}$$

Similarly, the inverse Fourier transform of the functions $\cos(n_x\Delta x k_x)\sin(n_y\Delta y k_y)$, $\sin(n_x\Delta x k_x)\cos(n_y\Delta y k_y)$ and $\sin(n_x\Delta x k_x)\sin(n_y\Delta y k_y)$ are :

$$\mathcal{F}^{-1}\{\cos(n_x\Delta x k_x)\sin(n_y\Delta y k_y)\} = -\frac{i}{4}(\delta_{-n_x,-n_y}-\delta_{-n_x,+n_y}+\delta_{+n_x,-n_y}-\delta_{+n_x,+n_y}), \quad \text{(B-7)}$$

$$\mathcal{F}^{-1}\{\sin(n_x\Delta x k_x)\cos(n_y\Delta y k_y)\} = -\frac{i}{4}(\delta_{-n_x,-n_y}+\delta_{-n_x,+n_y}-\delta_{+n_x,-n_y}-\delta_{+n_x,+n_y}), \quad \text{(B-8)}$$

$$\mathcal{F}^{-1}\{\sin(n_x\Delta x k_x)\sin(n_y\Delta y k_y)\} = -\frac{1}{4}(\delta_{-n_x,-n_y}-\delta_{-n_x,+n_y}-\delta_{+n_x,-n_y}+\delta_{+n_x,+n_y}). \quad \text{(B-9)}$$

Therefore the inverse Fourier transform of the functions $F^{ee}(k_x,k_y)$, $F^{oe}(k_x,k_y)$, $F^{eo}(k_x,k_y)$ and $F^{oo}(k_x,k_y)$ are:

$$\mathcal{F}^{-1}\{F^{ee}(k_x,k_y)\} = \sum_{n_x,n_y}\frac{1}{4}a^{ee}_{n_x,n_y}(\delta_{-n_x,-n_y}+\delta_{-n_x,+n_y}+\delta_{+n_x,-n_y}+\delta_{+n_x,+n_y}), \quad \text{(B-10)}$$

$$\mathcal{F}^{-1}\{F^{oe}(k_x,k_y)\} = \sum_{n_x,n_y}-\frac{i}{4}a^{oe}_{n_x,n_y}(\delta_{-n_x,-n_y}+\delta_{-n_x,+n_y}-\delta_{+n_x,-n_y}-\delta_{+n_x,+n_y}), \quad \text{(B-11)}$$

$$\mathcal{F}^{-1}\{F^{eo}(k_x,k_y)\} = \sum_{n_x,n_y}-\frac{i}{4}a^{eo}_{n_x,n_y}(\delta_{-n_x,-n_y}-\delta_{-n_x,+n_y}+\delta_{+n_x,-n_y}-\delta_{+n_x,+n_y}), \quad \text{(B-12)}$$

$$\mathcal{F}^{-1}\{F^{oo}(k_x,k_y)\} = \sum_{n_x,n_y}-\frac{1}{4}a^{oo}_{n_x,n_y}(\delta_{-n_x,-n_y}-\delta_{-n_x,+n_y}-\delta_{+n_x,-n_y}+\delta_{+n_x,+n_y}). \quad \text{(B-13)}$$

The correction operator $F(k_x,k_y)$ is the sum of $F^{ee}(k_x,k_y)$, $F^{oe}(k_x,k_y)$, $F^{eo}(k_x,k_y)$ and $F^{oo}(k_x,k_y)$. Therefore the inverse Fourier transform of the correction operator is:

$$\begin{aligned}
\mathcal{F}^{-1}\{F(k_x,k_y)\} &= \mathcal{F}^{-1}\{F^{ee}(k_x,k_y)\}+\mathcal{F}^{-1}\{F^{oe}(k_x,k_y)\}+\mathcal{F}^{-1}\{F^{eo}(k_x,k_y)\}+\mathcal{F}^{-1}\{F^{oo}(k_x,k_y)\} && \text{(B-14)}\\
&= \frac{1}{4}\sum_{n_x,n_y}(\delta_{-n_x,-n_y}c_{-n_x,-n_y}+\delta_{-n_x,+n_y}c_{-n_x,+n_y}+\delta_{+n_x,-n_y}c_{+n_x,-n_y}+\delta_{+n_x,+n_y}c_{+n_x,+n_y}) && \text{(B-15)}
\end{aligned}$$

where

$$\begin{aligned}
c_{-n_x,-n_y} &= [(a^{ee}_{n_x,n_y}-a^{oo}_{n_x,n_y})-i(a^{eo}_{n_x,n_y}+a^{oe}_{n_x,n_y})], && \text{(B-16)}\\
c_{-n_x,+n_y} &= [(a^{ee}_{n_x,n_y}+a^{oo}_{n_x,n_y})+i(a^{eo}_{n_x,n_y}-a^{oe}_{n_x,n_y})], && \text{(B-17)}\\
c_{+n_x,-n_y} &= [(a^{ee}_{n_x,n_y}+a^{oo}_{n_x,n_y})-i(a^{eo}_{n_x,n_y}-a^{oe}_{n_x,n_y})], && \text{(B-18)}\\
c_{+n_x,+n_y} &= [(a^{ee}_{n_x,n_y}-a^{oo}_{n_x,n_y})+i(a^{eo}_{n_x,n_y}+a^{oe}_{n_x,n_y})]. && \text{(B-19)}
\end{aligned}$$